Nucleic Acids Research, 1998, Vol. 26, No. 11 **2723–2728**

Mg^{2+} binding and structural stability of mature and *in vitro* synthesized unmodified *Escherichia coli* $tRNA^{Phe}$

Victor Serebrov[1,2], Konstantin Vassilenko[2], Natalya Kholod[3], Hans J. Gross[4] and Lev Kisselev[1,*]

[1]Engelhardt Institute of Molecular Biology, Moscow 117984, Russia, [2]Institute of Protein Research, Pushchino 142292, Russia, [3]Skryabin Institute of Biochemistry and Physiology of Microorganisms, Pushchino 142292, Russia and [4]Institut für Biochemie, Bayerische Julius-Maximilians-Universität, Biozentrum, Am Hubland, D-97074 Würzburg, Germany

Received January 28, 1998; Revised and Accepted April 22, 1998

ABSTRACT

Mature $tRNA^{Phe}$ from *Escherichia coli* and the transcript of its gene lacking modified nucleotides were compared by a variety of physical techniques. Melting experiments revealed that at a low Mg^{2+} level the transcript was partially denatured, while the mature tRNA possessed intact tertiary interactions. Mg^{2+} binding to both tRNAs was studied by CD and UV techniques as well as by using the Mg^{2+}-sensitive fluorescence indicator, 8-hydroxyquinoline 5-sulfonic acid. Both tRNA forms exhibited a single strong Mg^{2+}-binding site, its dissociation constant was 10-fold higher for the transcript. Conformational changes in response to Mg^{2+} addition measured by CD and UV spectrometry revealed no difference for the estimated binding cooperativity and strong differences for affinities of Mg^{2+}-binding sites for the two tRNA forms. Conformational transitions in mature and in *in vitro* synthesized tRNA required the binding of two Mg^{2+} ions per molecule and therefore should be associated not only with a single strong binding site. The Mg^{2+} dependence of Stokes radii measured by gel-filtration revealed insignificant differences between the overall sizes of the two tRNA forms at physiological Mg^{2+} levels (>1 mM). Taken together, these results suggest that modified nucleotides stabilize tertiary interactions and increase the structure stability without affecting the mechanism of Mg^{2+} binding and overall folding of the tRNA molecule. This conclusion is supported by the known biological activity of the *E.coli* $tRNA^{Phe}$ gene transcript.

INTRODUCTION

It is well known (1,2) that mature cellular tRNAs have a high content of up to 20% modified nucleosides. Apart from other functions, these odd elements probably stabilize the correct conformation of tRNA, thereby ensuring its specific recognition by various enzymes. By *in vitro* transcription, it became possible to obtain transcripts of tRNA genes without modified nucleosides. Comparison of mature tRNAs and transcripts lacking modification can contribute to the understanding of the role of modifications in formation of the three-dimensional tRNA structure.

After the first results on *in vitro* transcription of tRNA genes had been published (3,4), a large body of research was devoted to tRNA gene transcripts, mainly due to the possibility of applying powerful gene engineering tools in the tRNA field coupled with the observation that unmodified tRNA transcripts retained activity and exhibited kinetic parameters of the aminoacylation reaction close to those for native tRNAs (3,5,6). However, mature and unmodified tRNAs exhibited substantially different Mg^{2+} optima of aminoacylation (3). For mature and unmodified *Escherichia coli* $tRNA^{Thr}$ optimal Mg^{2+} concentrations are 5 and 8 mM, respectively (7). For mature and unmodified *E.coli* $tRNA^{Phe}$ these concentrations are 8 and 15 mM (N.Kholod, unpublished results). At relatively low Mg^{2+} concentration (3 mM), significant differences in the initial rates of aminoacylation were found for *E.coli* $tRNA^{Cys}$ and its transcript (8).

NMR studies performed for *E.coli* $tRNA^{Val}$ (9) and yeast $tRNA^{Phe}$ (4) and the corresponding unmodified transcripts demonstrated the similarity of mature and *in vitro* synthesized tRNA forms at high Mg^{2+} concentrations. In the absence or at a low level of Mg^{2+} the transcripts were shown to undergo structural rearrangement suggesting that they were unable to adopt the native conformation in these conditions. Unmodified *E.coli* $tRNA^{Val}$ exhibited disrupted contacts between the T- and D-loops and weakened strong Mg^{2+}-binding sites in the D-loop and near the D-stem. Analysis of the temperature dependence of the imino proton spectra showed that some tertiary interactions involving modified nucleotides in *E.coli* $tRNA^{Val}$ were less stable

*To whom correspondence should be addressed. Tel: +7 095 135 6009; Fax: +7 095 135 1405; Email: kissel@imb.imb.ac.ru

Dedicated to the memory of Professor Richard T. Walker

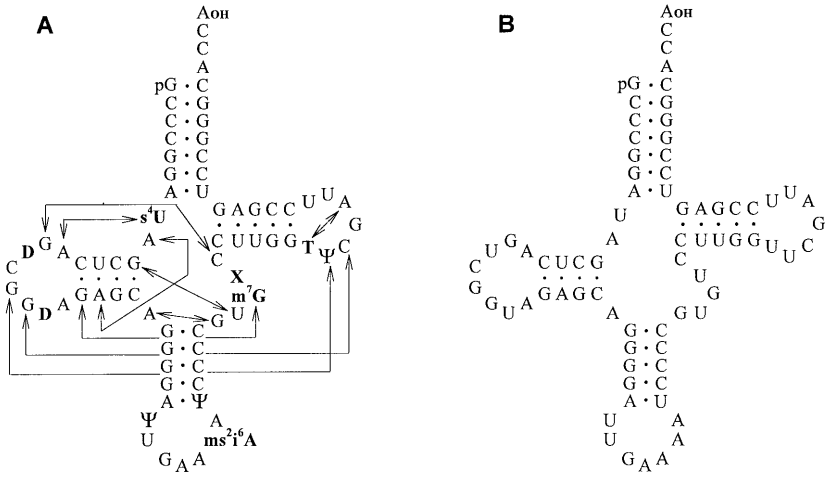

Figure 1. Primary and cloverleaf structures of $tRNA^{Phe}$ from *E.coli* (**A**) and its gene transcript (**B**). Modified nucleosides are shown in bold. Arrows show tertiary interactions known from the yeast $tRNA^{Phe}$ crystal structure (18).

in the absence of base modifications at high Mg^{2+} concentration. Modified nucleotides were found to be essential for the formation of a stable alternative temperature dependent conformation of the anticodon loop of native $tRNA^{Val}$. This conformation was not found in the unmodified tRNA transcript (10). Chemical probing revealed an increased sensitivity of the transcript molecule to cleavage by metal ions (11) and ribonucleases (11,12), indicating the complete or partial unfolding of the D-stem and disrupting the tertiary contacts between D- and T-loops. *In vitro* synthesized RNA duplexes containing s^2U and s^4U showed substantially altered thermal stability as compared with duplexes containing U in this position, suggesting significant structural changes (13).

Recent observations (14) demonstrated that base modification could prevent incorrect folding of the tRNA molecule. Probing of the solution structure of human mitochondrial $tRNA^{Lys}$ gene transcript revealed that in the presence of 10 mM Mg^{2+} this transcript does not fold into a cloverleaf structure but into an extended bulged hairpin. A single point mutation at nucleotide 9 designed to mimic the effect of m^1A present at position 9 in the native $tRNA^{Lys}$ was found to recover the cloverleaf folding. Interestingly, an extended bulged hairpin was a suboptimal structure generated for the tRNA molecule by computer software designed for predicting RNA folding (15).

The presence of bivalent metal ions, in particular magnesium, is an absolute requirement for the formation of tRNA spatial structure. Mg^{2+} ions substantially change tRNA solution structure when present at millimolar concentration. The angle between the anticodon and aminoacyl acceptor stems was shown to be strongly affected by elevation of Mg^{2+} concentration from 0 to 0.2 mM: the apparent interstem angle of yeast $tRNA^{Phe}$ was changed from 150 to 70° (16). A single base modification can influence Mg^{2+} binding to a local tRNA region thus affecting the entire tRNA structure (17).

In this study, mature $tRNA^{Phe}$ from *E.coli* and the transcript of its gene were compared by a variety of physical techniques. Figure 1 shows the primary and cloverleaf structures of mature $tRNA^{Phe}$ containing 10 modified nucleosides and of its gene transcript.

MATERIALS AND METHODS

$tRNA^{Phe}$ (*E.coli*) with the acceptor activity of 1400 pmol/A_{260} was purchased from Sigma. Denaturing PAGE showed at least 95% purity. Prior to measurements the samples were incubated at 95°C for 5 min in the presence of 1 mM EDTA and then ethanol-precipitated to remove traces of bivalent cations.

Plasmid pCF0 containing the $tRNA^{Phe}$ gene under control of the phage T7 promoter was linearized with restriction endonuclease *Bst*NI. Resulting DNA was used as a template for the run-off transcription reaction with phage T7 polymerase (19). $tRNA^{Phe}$ transcript was purified by preparative PAGE in the presence of 8 M urea.

Acceptor activity of the transcripts was measured as described elsewhere (20). After PAGE purification the tRNA gene transcript incorporated >1200 pmol phenylalanine/A_{260} unit of tRNA.

tRNA concentrations were determined by measuring optical density at 260 nm in water. Extinction coefficients (ε_{260}) for the mature tRNA and the transcript were determined as follows. To 0.6 ml of tRNA aqueous solution (0.5 A_{260}/ml) 0.3 U (1 µl) of nuclease P1 was added. After 3 h of incubation at 60°C an A_{260} of the digest was measured. Hyperchromic effect was determined from digested tRNA/native tRNA A_{260} ratio. The ε_{260} for tRNA digest was calculated using known ε_{260} for A, G, C and U and modified bases (21). Taking into account the hyperchromicity, 1 mg was found to be equivalent to 23.0 and 24.0 A_{260} units for the mature tRNA and the transcript, respectively. These values were used in all further calculations.

Experiments, if not indicated otherwise, were carried out at 37°C in a buffer containing 30 mM HEPES–KOH, pH 7.5 and 50 mM KCl.

Circular dichroism (CD) spectra were measured with a Jasco J-600 spectropolarimeter at a sample concentration of ~5 A_{260} U/ml using a 1 mm path-length CD cell (Jasco).

Melting profiles were obtained at 260 nm with a Cary 19 spectrophotometer equipped with a thermosensor and a water-jacketed cell holder connected to an external bath; a 1 mm cell

(Jasco) was used. To prevent evaporation during heating, silicon oil (Serva) was layered on the surface of the sample.

Magnesium titration experiments were performed with a Shimadzu UV-1601 spectrophotometer with a thermostated cell holder using a 10 mm path-length cell at ~1 A_{260} U/ml RNA concentration.

The Mg^{2+} binding to both forms of tRNA was measured using the fluorescence indicator 8-hydroxyquinoline 5-sulfonic acid (HQS). Fluorescence titrations were carried out with a lab-made spectrofluorimeter equipped with two monochromators from LOMO (Russia). Excitation and emission were at 350 and 500 nm, respectively, with 4 mm slit widths. The titrations were performed in 1 cm quartz cell (Hellma) by stepwise addition of small volumes of standard buffer containing 0.25 mM fluorescence indicator and 0.4 mM $MgCl_2$ to 1.0 ml of tRNA solution in the same buffer without Mg^{2+}. Titration of the indicator without tRNA was carried out similarly, and a calibration curve was plotted. Calculations of bound Mg^{2+} as well as fitting to Scatchard plots were performed as described elsewhere (22,23).

Gel filtration measurements of the Stokes radii were performed with a ToyoSoda TSK-2000SW HPLC column (0.75 × 60 cm) connected to the Pharmacia FPLC system. The column was water-jacketed and its temperature kept at 37°C using an external circulating bath. The flow rate was 0.5 ml/min in all experiments. Proteins with known molecular masses and Stokes radii were used to calibrate the column: horse cytochrome c, hen egg lysozyme and ovalbumin, bovine serum albumin and carbonic anhydrase B (all purchased from Sigma).

RESULTS

Melting experiments

Figure 2 shows differential melting curves for mature $tRNA^{Phe}$ and for an unmodified transcript of its gene based on changes in the absorbance at 260 nm at various Mg^{2+} concentrations. As seen from the Figure, mature $tRNA^{Phe}$ exhibits two distinct melting transitions in the absence of Mg^{2+}. The low-temperature transition at 30°C (peak I) is conventionally attributed to simultaneous melting of the D-arm and disruption of the tertiary contacts, while the high-temperature transition occurring at 53°C (peak II) corresponds to unfolding of the main part of the tRNA secondary structure (24). An increase of Mg^{2+} concentration causes a strong shift of the peak I towards higher temperatures. As the Mg^{2+} ion concentration increases to 0.1 mM or higher, a single melting transition is observed with the peak area close to the sum of the two peak areas for melting in the absence of Mg^{2+}, indicating that Mg^{2+} ions stabilize the tertiary structure and the D-stem (and apparently to some extent the whole secondary structure) in such a way that the entire structure melts by a two-state transition. On the contrary, for the transcript, the low-temperature transition was not observed (Fig. 2) suggesting that the transcript exhibits disrupted tertiary contacts and an unfolded D-stem in the absence of Mg^{2+}, unlike mature $tRNA^{Phe}$ which has intact tertiary interactions and all elements of the secondary structure below 30°C under these ionic conditions. Additionally, for mature tRNA melting, transition midpoints correspond to somewhat higher temperatures as compared with the transcript at all tested Mg^{2+} concentrations, reflecting a decreased overall stability of the transcript molecule lacking modified nucleosides. For the transcript, melting experiments cannot represent explicit evidence for tertiary structure formation upon

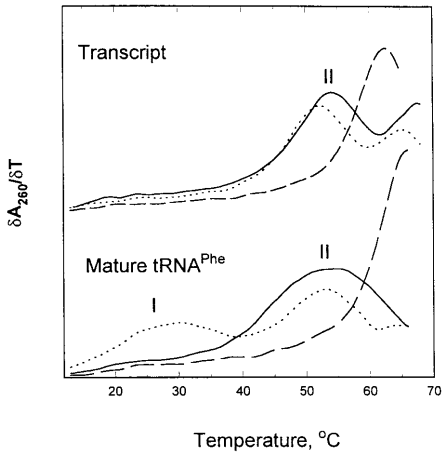

Figure 2. Differential melting curves for mature $tRNA^{Phe}$ and the transcript in buffer (30 mM HEPES–KOH, pH 7.5, 50 mM KCl) containing 0 mM (dotted line), 0.1 mM (solid line) and 2 mM (dashed line) $MgCl_2$. Melting transitions are indicated by peaks I and II.

Mg^{2+} addition, because the increase of peak II at 0.1 mM Mg^{2+} is not sufficient to prove the formation of complete tertiary structure.

For mature $tRNA^{Phe}$, the absence of peak I at 0.1 mM Mg^{2+} is evidence for strong stabilization of its tertiary structure by increasing the Mg^{2+} concentration from 0 to 0.1 mM, while the secondary structure melting point is only slightly affected (peak II). Further elevation of Mg^{2+} concentration to 2 mM strongly stabilizes the secondary structure of both tRNA forms. This indicates that Mg^{2+} binding to strong specific sites (saturating at <0.1 mM Mg^{2+}) can convert the tRNA molecule into a native-like form, while weak Mg^{2+}-binding sites are probably not involved in this process.

Fluorescence titration

The fluorescence indicator HQS is capable of measuring Mg^{2+} binding to tRNA (22). In order to obtain a reference curve, standard buffer containing 0.25 mM HQS was titrated with Mg^{2+}. HQS emission was plotted against Mg^{2+} concentration and used as a calibration plot (not shown). Although HQS has been reported to have a very low Mg^{2+} binding constant, a significant amount of added Mg^{2+} appeared to bind to HQS at 0.25 mM HQS concentration, which causes non-linearity of the calibration plot. Therefore, the experimental calibration plot for Mg^{2+} binding to HQS was fitted according to the theoretical Scatchard equation for 1:1 stoichiometry of the HQS–Mg^{2+} complex formation and the resulting curve was applied for determination of bound Mg^{2+} in tRNA titration experiments.

Experimental Scatchard plots for Mg^{2+} binding to mature tRNA and its transcript are shown in Figure 3. The fitting of the experimental points was performed for a conventional tRNA model possessing two classes of non-interacting Mg^{2+}-binding sites (25).

Unexpectedly, these plots appeared to be not simply biphasic but of a more complex nature. They have a distinct bulge at $\nu = 6$ for mature tRNA and at $\nu = 10$ for the transcript, where ν is the ratio of [occupied sites]/[all sites]. This feature was reproducibly observed in several experiments and indicates a cooperativity of Mg^{2+} binding occurring at the intermediate Mg^{2+} concentration

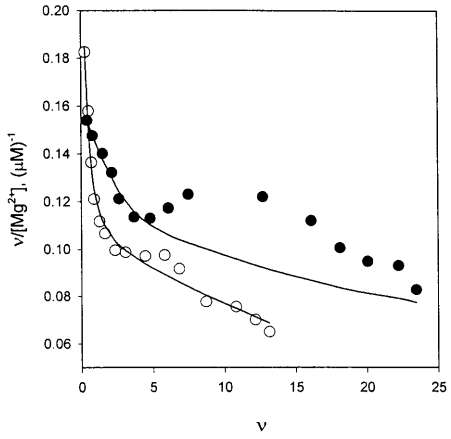

Figure 3. Scatchard plots for the binding of Mg^{2+} to mature $tRNA^{Phe}$ (open symbols) and to the transcript (filled symbols). Curves (solid lines) represent the fits according to the model of two classes of non-interacting sites (23,26). For the transcript, the region of cooperativity was neglected in calculations.

range. For the transcript this effect is more clearly defined than for mature tRNA. It should be mentioned that for the transcript this type of plot is associated with very low accuracy in determining binding parameters even if the bulged region is neglected.

The fitness of experimental data according to the Scatchard equation (23) showed the presence of a single strong Mg^{2+}-binding site for mature tRNA as well as for the transcript defined from calculated binding parameters for strong sites. The best fit for the mature tRNA was obtained at a value of 0.9 ± 0.2 and at 1.0 ± 0.6 for the transcript. In this latter case, experimental points at $\nu < 5$ were used for calculations and binding parameters were determined only for strong Mg^{2+}-binding sites. The corresponding binding constants are $k_{s(m)} = (7.5 \pm 3.8) \times 10^5\ M^{-1}$ and $k_{s(t)} = (5 \pm 3) \times 10^4\ M^{-1}$ for mature $tRNA^{Phe}$ and its transcript, respectively. Mature tRNA exhibits 30 ± 5 weak Mg^{2+}-binding sites with binding constant $k_{w(m)} = (2.4 \pm 0.5) \times 10^3\ M^{-1}$, while the corresponding parameters for the transcript could not be accurately determined.

It should be pointed out that the model of two classes of non-interacting Mg^{2+}-binding sites applied in the above calculations does not consider cooperative effects observed experimentally, particularly for the transcript (Fig. 3). This non-fitness concerns mainly the part of the plots which represents saturation of weak magnesium binding sites. Nevertheless, this model is able to define, at least partly, the binding parameters. A more satisfactory model that considers cooperative effects occurring at intermediate Mg^{2+} concentrations has to be elaborated in future.

Magnesium binding monitored by UV and CD techniques

UV and CD spectrometry permit the indirect monitoring of conformational transitions following binding of a ligand by measuring hyperchromicity and ellipticity effects. We have used these techniques to follow conformational changes occurring upon Mg^{2+} addition to the mature $tRNA^{Phe}$ and the transcript. The amplitude of CD spectra changes is ~1.5-fold larger for the transcript and suggests that the transcript undergoes greater structural changes upon Mg^{2+} binding in comparison with the mature tRNA. Some shift of CD band observed during titration

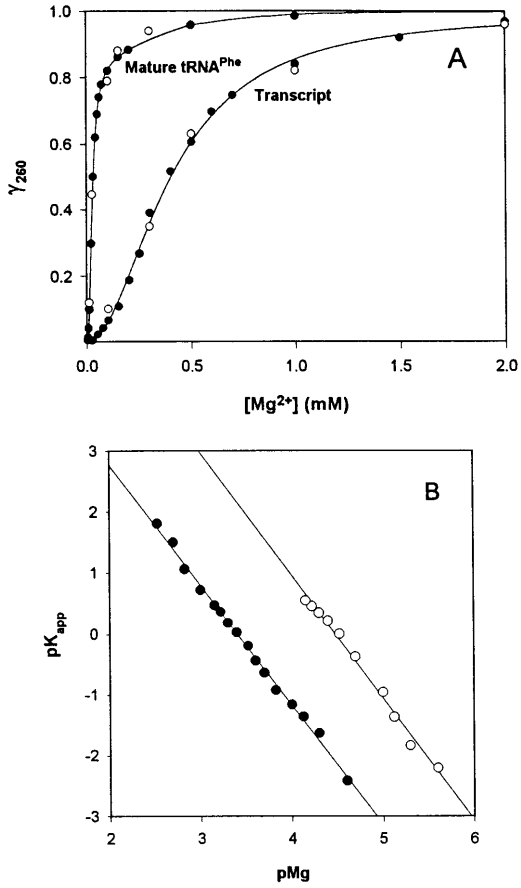

Figure 4. (**A**) Magnesium-induced hyperchromicity (filled symbols) and ellipticity (open symbols) at 260 nm for mature $tRNA^{Phe}$ and the transcript normalized for sample concentration (γ_{260}) plotted versus Mg^{2+} concentration. (**B**) Plots of $\log\{(1 - \theta)/\theta\}$ versus pMg based on the data from (A) for mature tRNA (open symbols) and the transcript (filled symbols). Straight lines represent linear regression.

for the transcript can be accounted for by the absence of the modified nucleoside contribution (data not shown).

A great difference in affinity for Mg^{2+} ions was observed for the two forms of tRNA. As seen from titration curves (Fig. 4A), absorbance and CD data closely coincide. The shapes of both curves are similar and indicative of a cooperative mechanism of Mg^{2+}-induced conformational transitions for mature $tRNA^{Phe}$ as well as for the transcript. For these curves, the midpoint Mg^{2+} concentrations differ dramatically. The transition midpoint is ~0.05 mM Mg^{2+} for mature $tRNA^{Phe}$, while it is 10-fold higher for unmodified transcript. The data presented in Figure 4A can be quantified by the semi-empirical Hill equation for the binding of n Mg^{2+} ions to tRNA

$$nMg^{2+} + tRNA \leftrightarrow tRNA{\cdot}Mg^{2+}{}_n$$

$$K_{app}{}^n = [tRNA][Mg^{2+}]^n/[tRNA{\cdot}Mg^{2+}{}_n] = (1 - \theta)[Mg^{2+}]^n/\theta$$

and

$$\log\{(1 - \theta)/\theta\} + n{\cdot}pK_{app} = n{\cdot}pMg^{2+} \qquad \mathbf{1}$$

where K_{app} is a dissociation constant for the $tRNA{\cdot}Mg_n$ complex, θ is the ratio of $[tRNA{\cdot}Mg^{2+}{}_n]$ to $[tRNA]_{total}$, and n is an empirical Hill coefficient of cooperativity. Assuming that at

2.4 μM tRNA concentration $[Mg^{2+}]_{free} \cong [Mg^{2+}]_{total}$, this equation can be applied to our experimental data. Figure 4B shows plots of $\log\{(1 - \theta)/\theta\}$ versus pMg for mature tRNA and the transcript. The data fit well to equation **1** over the entire range of θ for the transcript and over $0 < \theta < 0.7$ for mature $tRNA^{Phe}$. We have obtained n = 1.97 for the transcript and n = 2.01 for mature $tRNA^{Phe}$. This suggests the existence of two cooperatively interacting Mg^{2+}-binding sites for both tRNA forms. K_{app} is more than one order of magnitude less for the transcript than for mature $tRNA^{Phe}$ as follows from pK_{app} values calculated from the data shown in Figure 4B. They were found to be equal to 3.36 and 4.50 for the transcript and mature tRNA, respectively. The corresponding values of the stability constants are $k_{tr} = 2.29 \times 10^3\ M^{-1}$ and $k_{mat} = 3.16 \times 10^4\ M^{-1}$, reflecting significant differences in Mg^{2+} binding affinities between the two tRNA forms.

Mg^{2+}-induced changes of Stokes radii

The Stokes radius (R_s) is a hydrodynamic parameter of a molecule which is sensitive to large conformational rearrangements leading to significant changes in the overall size of a molecule. We have used a simple and accurate gel-filtration technique for determining Mg^{2+} concentration dependence of R_s for mature and unmodified tRNA forms. This technique is widely applied for proteins (26).

Proteins with known R_s were used to calibrate the column (see Materials and Methods). Plotting of inverse retention volumes versus logarithmic values of protein R_s yielded a calibration plot fitting well to linear regression (data not shown). Measurement of a retention volume for the tRNA sample in buffer containing variable Mg^{2+} concentrations gives an R_s value derived from the calibration plot (27).

Figure 5 presents gel-filtration data on Mg^{2+}-induced changes in the overall dimensions of mature and unmodified $tRNA^{Phe}$. As one can see, both tRNA forms shrink drastically upon increasing Mg^{2+} concentration to 15 mM. The corresponding values of R_s reduces from 3.4 to 2.5 nm due to Mg^{2+}-induced phosphate group screening and loss of charges. Another remarkable feature of these curves is that they are in fact indistinguishable. A small difference is observed only at relatively low Mg^{2+} concentrations: mature $tRNA^{Phe}$ is slightly more compact and its R_s drops slightly faster with increasing magnesium concentration than for the transcript. The latter could reflect the differences in Mg^{2+} concentrations required for conformational changes seen by spectral methods for the two tRNA forms (Fig. 4A).

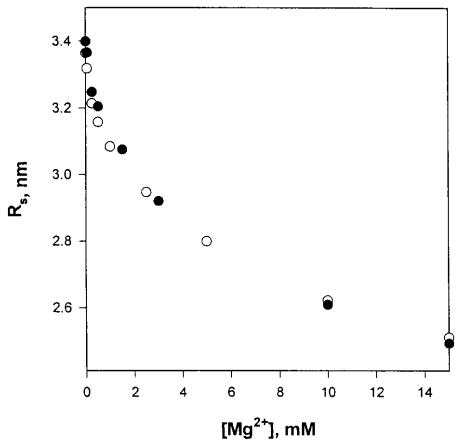

Figure 5. The Mg^{2+} concentration dependence of Stokes radii for mature $tRNA^{Phe}$ (open symbols) and the transcript (filled symbols) derived from gel-filtration experiments.

DISCUSSION

As follows from melting experiments (Fig. 2), the tertiary contacts and the D-arm are intact in the modified tRNA below 30°C in the absence of Mg^{2+}, while the transcript, being partially denatured, lacks these structural elements. The secondary and tertiary structures of mature tRNA prove to be more stable at various Mg^{2+} concentrations, as follows from comparison of their melting temperatures. During Mg^{2+}-induced transition the amplitude of spectral effects of the transcript is broader and indicative of greater structural changes occurring during the conversion into the native-like conformation. The stability constant of the strong Mg^{2+}-binding site of mature $tRNA^{Phe}$ seems to be considerably higher than for the transcript. The Mg^{2+}-induced conformational transition observed in the above experiments can be attributed to formation of the tertiary structure and conversion of tRNA molecule into the completely folded form. As seen from melting experiments, at 37°C in the absence of Mg^{2+} ions, tertiary structure and D-stem are melted in mature tRNA as well as in the transcript (Fig. 2). For mature tRNA at this temperature, elevation of Mg^{2+} concentration to 0.1 mM leads to the formation of tertiary structure. For the transcript, at least a 10-fold higher Mg^{2+} concentration is required (Fig. 4A). Therefore, Mg^{2+}-induced spectral effects are associated with formation of tertiary structure caused by Mg^{2+} binding to tRNA molecules and accompanied by formation of new base pairs and increase of the base stacking. At high Mg^{2+} concentration secondary structure probably contributes to the measured hyperchromicity effects. The cooperative dependence of hyperchromicity on Mg^{2+} concentration indicates that two interacting magnesium binding sites exist in both tRNA forms. The significant difference in the Mg^{2+} concentrations required for conformational transitions of the two tRNA forms (Fig. 4A) accounts for the differences between the stability constants of the Mg^{2+}-binding sites.

Fluorescence titration experiments help to distinguish the types of Mg^{2+}-binding sites in the tRNA molecule. As seen from Figure 3, a single strong Mg^{2+}-binding site was found in both tRNA forms under the given experimental conditions. However, the cooperative effects observed in these experiments imply the existence of at least two Mg^{2+}-binding sites. Apparently, Mg^{2+} binding to the single strong site does not cause conformational changes monitored by spectral techniques. This assumption is supported by the observation that the binding constants derived from spectral measurements are about one order of magnitude higher than those calculated for the single strong Mg^{2+}-binding site by fluorescence titration, both for the mature tRNA and for the transcript. Conformational transition is probably induced by cooperative binding of Mg^{2+} ions to two sites possessing an intermediate affinity and corresponding to bulges seen on Scatchard plots at intermediate Mg^{2+} concentrations (Fig. 3).

Non-coincidence of our data with those available for the Scatchard plots for binding of the bivalent ions to yeast $tRNA^{Phe}$ (22,25,28) probably originated from the different ionic conditions. Scatchard plots for Mg^{2+} binding to $tRNA^{Phe}$ exhibited no cooperative effects at low ionic strength, while in our experiments at relatively high monovalent ion concentration (80 mM K^+)

these plots clearly indicate cooperativity of the binding. Our Scatchard plots for Mg^{2+} binding to the yeast $tRNA^{Phe}$ at high ionic strength demonstrated cooperativity and reduced number of strong Mg^{2+}-binding sites with reduced affinity (data not shown).

Conformational changes revealed by spectral methods at low Mg^{2+} concentrations did not contribute significantly to the R_s changes. The latter took place at much higher Mg^{2+} concentrations.

The results obtained suggest that the folding and molecular size are governed by the primary structure which is similar for both forms of tRNA (Fig. 1). The observed differences concern only magnitudes of specific binding parameters such as stability constants of magnesium binding sites, but apparently neither type of magnesium binding nor molecular mechanism of the conversion into the completely folded form is caused by added Mg^{2+}. As mentioned above, in some cases (14) modified nucleosides are able to prevent incorrect folding of the tRNA molecule. Therefore, the role of modified bases is probably to fix the correct conformation of local regions of the tRNA molecule so that they readily adopt specific conformation converting the molecule into the native state. In line with this suggestion, the modified nucleosides in mature tRNA could provide high binding constants for strong Mg^{2+}-binding sites. The presumable loci of such action are the D-loop and the contact between the D- and T-loops. This region has been shown to be responsible for the formation of the native tRNA structure (10–12). Moreover, as seen from the crystal structure of yeast $tRNA^{Phe}$ (29), it has an unusual RNA chain topology where a strong Mg^{2+}-binding site exists, and Mg^{2+} ion bound to this site plays the role of a molecular bridge between proximal segments of D- and T-loops.

Though significant structural difference was noticed between mature and *in vitro* synthesized tRNA forms at low Mg^{2+} concentration, this difference diminishes upon increasing the magnesium concentration to the physiological level. The types of Mg^{2+} binding seem to be similar for both forms. The transcript was found to adopt a less folded conformation as compared with the mature form. This feature is reflected in weakened affinities of specific Mg^{2+}-binding sites of the transcript. The excess of Mg^{2+} compensates, at least partly, for the absence of modified nucleotides in the transcript.

ACKNOWLEDGEMENTS

We are grateful to O.Uhlenbeck for his kind gift of plasmid pCF0. We thank O.Ptitsyn and V.Ksenzenko for critical reading of the manuscript and valuable comments, and E.Gupalo for assistance in preparation of the manuscript. This work was supported by the Volkswagen Foundation (project ‘tRNA folding’) and by the Russian Foundation for Basic Research.

REFERENCES

1 Bjork,G. (1995) In Söll,D. and RajBhandary,U. (eds), *tRNA: Structure, Biosynthesis, and Function*. ASM Press, Washington, DC, pp. 165–206.
2 Yokoyama,S. and Nishimura,S. (1995) In Söll,D. and RajBhandary,U. (eds), *tRNA: Structure, Biosynthesis, and Function.* ASM Press, Washington, DC, pp. 207–224.
3 Sampson,J. and Uhlenbeck,O. (1988) *Proc. Natl. Acad. Sci. USA*, **85**, 1033–1037.
4 Hall,K., Sampson,J., Uhlenbeck,O. and Redfield,A. (1989) *Biochemistry*, **14**, 5794–5801.
5 McClain,W. (1995) In Söll,D. and RajBhandary,U. (eds), *tRNA: Structure, Biosynthesis, and Function.* ASM Press, Washington, DC, pp. 335–348.
6 Pallank,L., Pak,M. and Schulman,L. (1995) In Söll,D. and RajBhandary,U. (eds), *tRNA: Structure, Biosynthesis, and Function.* ASM Press, Washington, DC, pp. 371–394.
7 Schulman,L. and Pelka,H. (1990) *Nucleic Acids Res.*, **18**, 285–289.
8 Komatsoulis,G. and Abelson,J. (1993) *Biochemistry*, **32**, 7435–7444.
9 Yue,D., Kintanar,A. and Horowitz,J. (1994) *Biochemistry*, **33**, 8905–8911.
10 Derrick,W. and Horowitz,J. (1993) *Nucleic Acids Res.*, **21**, 4948–4953.
11 Michakowski,D., Wrzesinski,J. and Krzysosiak,W. (1996) *Biochemistry*, **35**, 10727–10734.
12 Michakowski,D., Wrzesinski,J., Ciesioska,J. and Krzysosiak,W. (1996) *Biochimie*, **78**, 131–138.
13 Kumar,R. and Davis,D. (1997) *Nucleic Acids Res.*, **25**, 1272–1280.
14 Helm,M., Brule,H., Degoul,F., Cepanec,C., Leroux,J.-P., Giege,R. and Florentz,C. (1998) *Nucleic Acids Res.*, **26**, 1636–1643.
15 Zuker,M. and Stiegler,P. (1981) *Nucleic Acids Res.*, **9**, 133–148.
16 Friederich,M. and Hagerman,P. (1997) *Biochemistry*, **36**, 6090–6099.
17 Lam,A., Guenther,R. and Agris,P. (1995) *Biometals*, **8**, 290–296.
18 Hollbrook,S., Sussman,J., Warrant,R. and Kim,S. (1978) *J. Mol. Biol.*, **123**, 631–660.
19 Peterson,E. and Uhlenbeck,O. (1992) *Biochemistry*, **31**, 10380–10389.
20 Kholod,N., Pan’kova,N., Mayorov,S., Krutilina,A., Shlyapnikov,M., Kisselev,L. and Ksenzenko,V. (1997) *FEBS Lett.*, **411**, 123–127.
21 Dawson,R., Elliott,D., Elliott,W. and Jones,K. (1986) *Data For Biochemical Research*. Clarendon Press, Oxford.
22 Romer,R. and Hach,R. (1975) *Eur. J. Biochem.*, **55**, 271–284.
23 Scatchard,G. (1949) *Ann. N.Y. Acad. Sci.*, **51**, 660–672.
24 Draper,E. (1996) *Trends Biochem. Sci.*, **21**, 145–149.
25 Schreier,A. and Schimmel,P. (1974) *J. Mol. Biol.*, **86**, 601–620.
26 Uversky,V. (1993) *Biochemistry*, **32**, 13288–13298.
27 Ackers,G. (1967) *J. Biol. Chem.*, **242**, 3026–3034.
28 Leroy,J. and Gueron,M. (1977) *Biopolymers*, **16**, 2429–2446.
29 Holbrook,S., Sussman,J., Warrant,R., Church,G. and Kim,S.-H. (1977) *Nucleic Acids Res.*, **4**, 2811–2820.